CIB-W18/38-7-4

INTERNATIONAL COUNCIL FOR RESEARCH AND INNOVATION IN BUILDING AND CONSTRUCTION

WORKING COMMISSION W18 - TIMBER STRUCTURES

SELF-TAPPING SCREWS AS REINFORCEMENTS IN CONNECTIONS WITH DOWEL-TYPE FASTENERS

I Bejtka

H J Blaß

Universität Karlsruhe

GERMANY

MEETING THIRTY-EIGHT

KARLSRUHE

GERMANY

AUGUST 2005

Self-tapping screws as reinforcements in connections with dowel-type fasteners

I. Bejtka, H.J. Blaß
Lehrstuhl für Ingenieurholzbau und Baukonstruktionen
Universität Karlsruhe, Germany

1 Introduction

Connections with dowel-type fasteners are often used to transfer loads between timber members. Here, the load-carrying capacity, which can be calculated according to Johansen´s yield theory, is limited by the embedding strength of the timber, by the yield moment of the dowel-type fasteners and finally by the geometry of the connection.

The spacing of dowel-type fasteners affects the splitting tendency of timber in the connection area. The splitting tendency increases with decreasing fastener spacing parallel to the grain and hence decreases the effective number of fasteners n_{ef}. Splitting may be prevented by reinforcing the connection area and, consequently, the effective number n_{ef} of fasteners increases. Self-tapping screws with continuous threads represent a simple and economic reinforcement method. The screws are placed between the dowel-type fasteners, both perpendicular to the dowel axis and to the grain direction.

In connections with sufficient reinforcement between the dowels, the timber does not split and the effective number n_{ef} equals the actual number n of dowels.

Timber splitting is prevented, when the axial load-carrying capacity R_{ax} of each screw is larger than 30% of the lateral load-carrying capacity R per shear plane of each dowel [1]. The lateral load-carrying capacity R can be calculated according to Johansen´s yield theory. The axial load-carrying capacity R_{ax} of the screws may e.g. be calculated according to [2].

Furthermore, by placing the screws in contact with the dowel-type fasteners (Fig. 1), the load-carrying capacity and the stiffness of a connection increases.

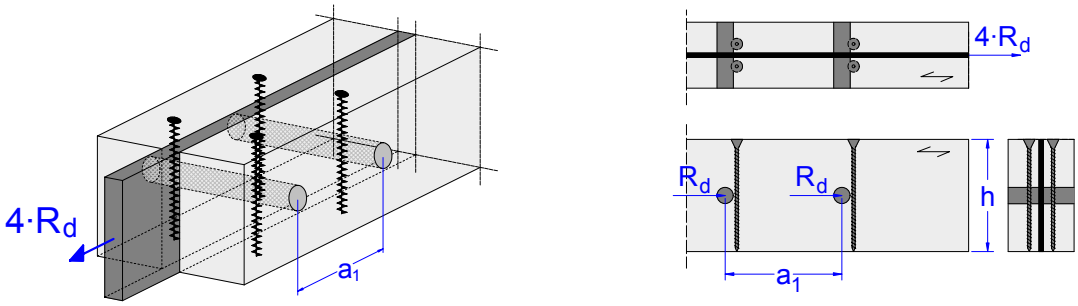

Fig. 1: Reinforced connection using self-tapping screws placed in contact with the dowels

Both effects – preventing splitting and increasing the load-carrying capacity by placing the screws in contact with the dowels – may cause an increase of up to 120% of the load-carrying capacity compared to non-reinforced connections (Fig. 2).

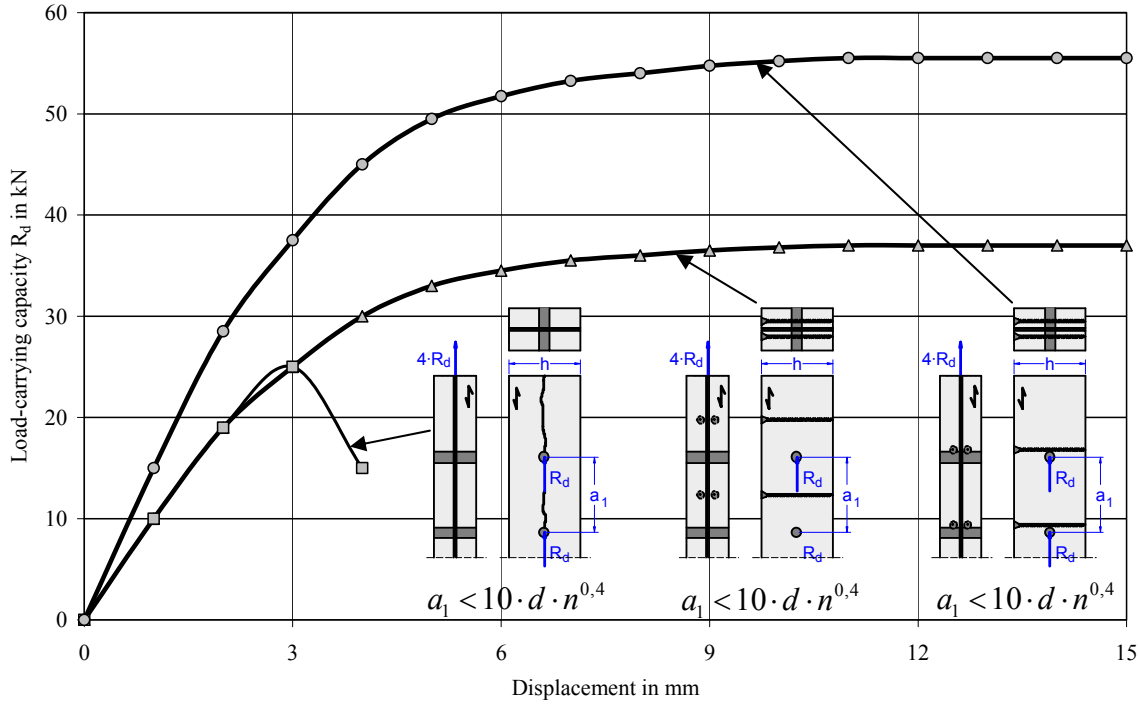

Fig. 2: Typical load-displacement-curves of non-reinforced and reinforced connections

A calculation model as an extension of Johansen´s yield theory and based on theoretical and experimental studies is presented.

2 Calculation model for the extended Johansen´s yield theory

2.1 Assumptions

The load-carrying capacity for reinforced connections is derived on the basis of the same assumptions as Johansen´s yield theory. The screws, placed in contact with the dowel-type fasteners, perpendicular to the dowel axis and to the grain direction (Fig. 1), are loaded just as the dowels themselves perpendicular to their axis. One of the basic assumptions in Johansen´s yield theory is an ideal rigid-plastic material behaviour of the timber in embedding and of the fastener in bending. Under this assumption, screws as reinforcements loaded perpendicular to their axis also show an ideal rigid-plastic load-carrying behaviour (Fig. 3).

Consequently, the screw only moves in force direction, when the dowel load component F_{VE} reaches the load-carrying capacity R_{VE} of the screw. In this case, the screw represents a “soft” support. Alternatively, for $F_{VE} < R_{VE}$, the screw does not move and represents a rigid support for the dowel. This consideration leads to four sub-failure modes for each failure mode in timber-to-timber connections and two sub-failure modes for each failure mode in steel-to-timber connections in Johansen´s yield theory. Subsequently, the sub-

failure modes for reinforced steel-to-timber and timber-to-timber connections are presented.

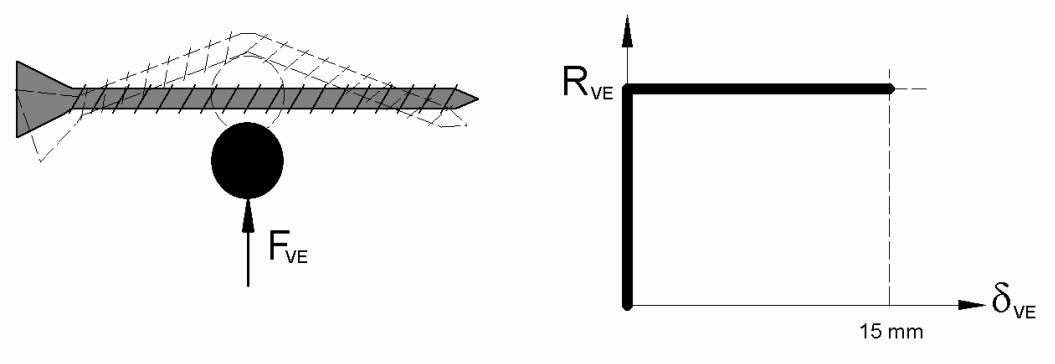

Fig. 3: Assumed load-carrying behaviour of a screw as reinforcement loaded perpendicular to the axis

2.2 Reinforced steel-to-timber connections

As an example for the derivation of all failure modes, the load-carrying capacity for a reinforced steel-to-timber connection with an inner steel plate and with two plastic hinges (failure mode 3) per shear plane is derived. The load-carrying capacity for the corresponding non-reinforced connection (right side in Fig. 4) is derived from the force and moment equilibrium in the shear plane (see equation (1)).

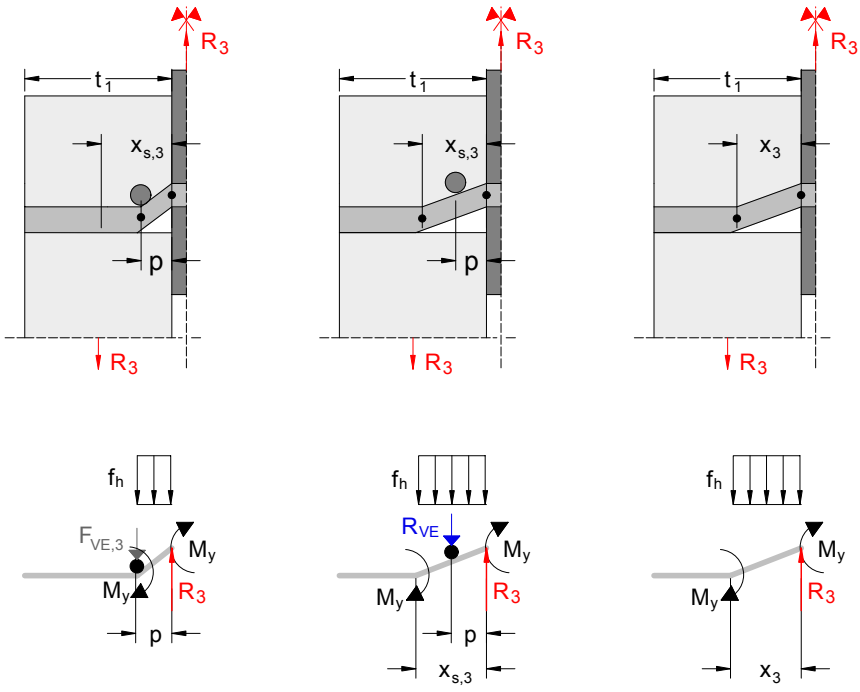

Fig. 4: Reinforced connection with sub-failure mode “rigid”, reinforced connection with sub-failure mode “soft” and non-reinforced connection (from left to right side)

$$R_3 = \sqrt{2} \cdot \sqrt{2 \cdot M_y \cdot f_h \cdot d} \tag{1}$$

The distance x_3 between the shear plane and the plastic hinge is given in equation (2).

$$x_3 = \sqrt{\frac{4 \cdot M_y}{f_h \cdot d}} \tag{2}$$

By placing the screws in contact with the dowel in-between the shear plane and the plastic hinge for a non-reinforced connection ($p < x_3$) and taking into consideration the load-carrying behaviour of the screw (Fig. 3), two sub-failure modes for failure mode 3 can occur (left and middle side in Fig. 4).

Sub-failure mode "rigid" appears for $F_{VE,3} < R_{VE}$. R_{VE} is the lateral load-carrying capacity of the screw. $F_{VE,3}$ can be derived from the force and moment equilibrium in the shear plane for the left system in Fig. 4 (eq. (3)).

$$F_{VE,3} = \frac{2 \cdot M_y}{p} - \frac{f_h \cdot d \cdot p}{2} \tag{3}$$

In this case, the load-carrying capacity R_3 is derived as:

$$R_3 = \frac{2 \cdot M_y}{p} + \frac{f_h \cdot d \cdot p}{2} \tag{4}$$

In the case of $F_{VE,3} \geq R_{VE}$ the load-carrying capacity of a reinforced connection is derived from the force and moment equilibrium in the shear plane for the middle system in Fig. 4 (sub-failure mode "soft") as:

$$R_3 = R_{VE} + \sqrt{2} \cdot \sqrt{f_h \cdot d \cdot \left(2 \cdot M_y - R_{VE} \cdot p\right)} \tag{5}$$

Recapitulating, the load-carrying capacity for Johansen's failure mode 3 for a reinforced steel-to-timber connection can be calculated as follows:

For $p \geq x_3$ no reinforcement occurs. The load-carrying capacity for failure mode 3 is calculated according to eq. (1).

For $p < x_3$ the reinforcement increases the load-carrying capacity. For $F_{VE,3} < R_{VE}$ the load-carrying capacity is calculated according to eq. (4), for $F_{VE,3} \geq R_{VE}$ according to eq. (5). $F_{VE,3}$ for failure mode 3 is calculated using eq. (3).

Similarly, the load-carrying capacities of the other two failure modes for reinforced steel-to-timber connections with an inner steel plate are derived. Therewith, the load-carrying capacity for reinforced steel-to-timber connections with an inner steel plate can be calculated as follows.

$$R = \min\left\{R_1, R_2, R_3\right\} \tag{6}$$

with

$$R_1 = f_h \cdot d \cdot t_1 + R_{VE} \tag{7}$$

$$R_2 = f_h \cdot d \cdot t_1 \cdot \left[\sqrt{2 + \frac{4}{t_1^2} \cdot \frac{M_y}{f_h \cdot d}} - 1\right] \qquad \text{for } p \geq x_2 \tag{8}$$

$$R_2 = \frac{M_y}{p} + f_h \cdot d \cdot t_1 \cdot \left[\frac{t_1}{2 \cdot p} + \frac{p}{t_1} - 1\right] \qquad \text{for } p < x_2 \text{ and } R_{VE} > F_{VE,2} \tag{9}$$

$$R_2 = R_{VE} + f_h \cdot t_1 \cdot d \cdot \left[\sqrt{2 + \frac{4}{t_1^2} \cdot \left(\frac{M_y - R_{VE} \cdot p}{f_h \cdot d} \right)} - 1 \right] \quad \text{for } p < x_2 \text{ and } R_{VE} \le F_{VE,2} \tag{10}$$

$$\text{with } F_{VE,2} = \frac{M_y}{p} + \frac{f_h \cdot d}{p} \cdot \left[\frac{t_1^2}{2} - p^2 \right] \quad \text{and } x_2 = \sqrt{\frac{t_1^2}{2} + \frac{M_y}{f_h \cdot d}} \tag{11}$$

$$R_3 = \sqrt{2} \cdot \sqrt{2 \cdot M_y \cdot f_h \cdot d} \quad \text{for } p \ge x_3 \tag{12}$$

$$R_3 = \frac{2 \cdot M_y}{p} + \frac{f_h \cdot d \cdot p}{2} \quad \text{for } p < x_3 \text{ and } R_{VE} > F_{VE,3} \tag{13}$$

$$R_3 = R_{VE} + \sqrt{2} \cdot \sqrt{f_h \cdot d \cdot \left(2 \cdot M_y - R_{VE} \cdot p \right)} \quad \text{for } p < x_3 \text{ and } R_{VE} \le F_{VE,3} \tag{14}$$

$$\text{with } F_{VE,3} = \frac{2 \cdot M_y}{p} - \frac{f_h \cdot d \cdot p}{2} \quad \text{and } x_3 = \sqrt{\frac{4 \cdot M_y}{f_h \cdot d}} \tag{15}$$

Fig. 5 shows the reinforcing effect as a R over R_{VE} diagram for a steel-to-timber connection with a 16 mm steel dowel, for an embedding strength f_h = 30 N/mm^2, a yield moment M_y = 246 Nm, a timber member thickness t_1 = 60 mm and a distance p = 20 mm.

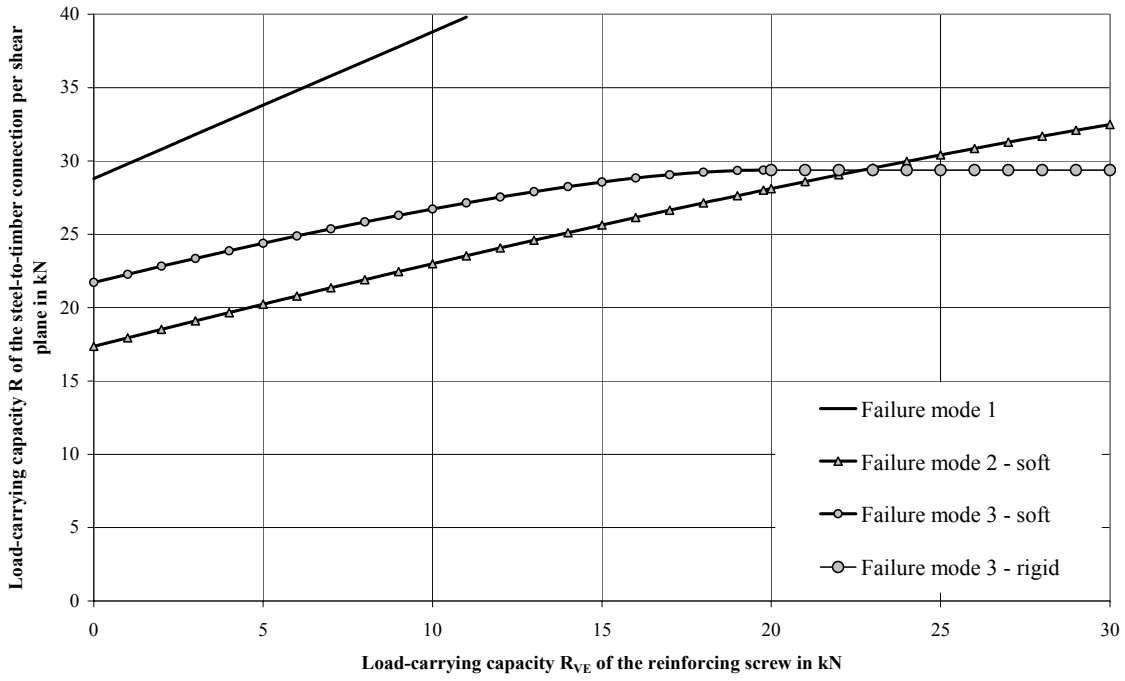

Fig. 5: Load-carrying capacity R for a steel-to-timber connection depending on R_{VE}

For R_{VE} = 0 the load carrying capacity R is equal to the load-carrying capacity for a non-reinforced connection (R = 17,4 kN). Here, failure mode 2 with one plastic hinge per shear plane occurs. With increasing load-carrying capacity R_{VE} of the screw, the load-carrying capacity R of the steel-to-timber connection increases. For R_{VE} = 22,6 kN the load-carrying capacity R reaches the maximum value of about R = 29,4 kN which is equal to an increase of about 69%. Due to the fact that for even higher values of R_{VE} sub-failure mode "rigid" occurs, a further increase is not possible.

2.3 Reinforced timber-to-timber connections

Compared to reinforced steel-to-timber connections, the calculation model for reinforced timber-to-timber connections is more complicated. In addition to the presented sub-failure modes "rigid" and "soft", two further sub-failure modes "rigid-soft" and "soft-rigid" for each Johansen´s failure mode occur. These additional sub-failure modes occur, when the load-carrying capacities for the reinforcements $R_{1,VE}$ and $R_{2,VE}$ or/and the load components $F_{1,VE}$ and $F_{2,VE}$ in both timber members are not equal. $R_{1,VE} \neq R_{2,VE}$ or/and $F_{1,VE} \neq F_{2,VE}$, when the timber density ρ in both timber members is not equal.

As an example for the derivation of all failure modes, the load-carrying capacity for a reinforced timer-to-timber connection with two plastic hinges per shear plane (failure mode 3) is derived. All possible sub-failure modes for Johansen's failure mode 3 are shown in Fig. 6.

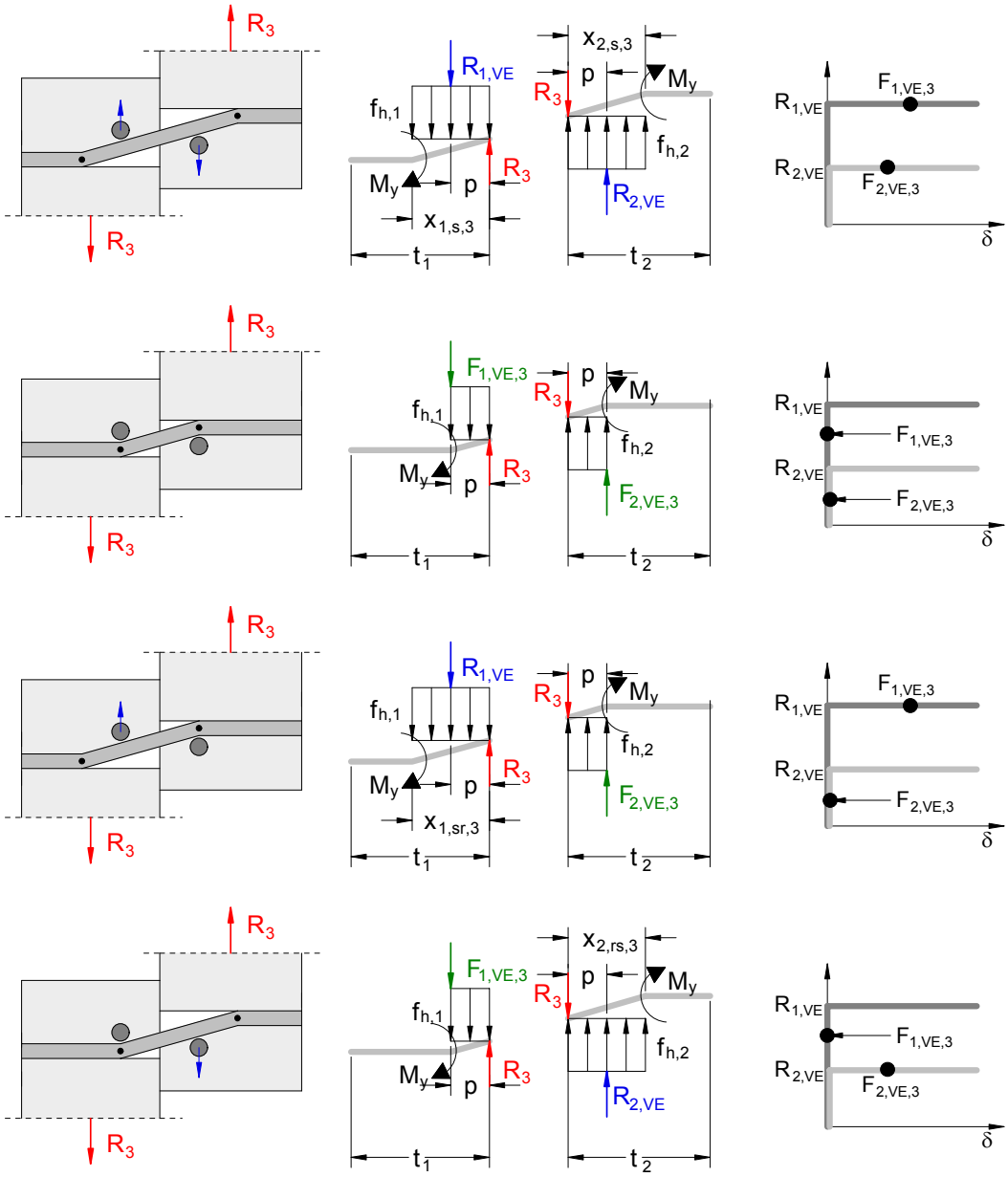

Fig. 6: Reinforced timber-to-timber connection with sub-failure modes "soft", "rigid", "soft-rigid" and "rigid-soft" for Johansen's failure mode 3 (from top to bottom)

The load-carrying capacity for the non-reinforced connection is derived from the force and moment equilibrium in the shear plane as:

$$R_3 = \frac{\sqrt{2 \cdot \beta}}{\sqrt{1+\beta}} \cdot \sqrt{2 \cdot M_y \cdot f_{h,1} \cdot d} \tag{16}$$

The distances $x_{1,3}$ and $x_{2,3}$ between the shear plane and the plastic hinges for a non-reinforced connection are:

$$x_{1,3} = \sqrt{\frac{2 \cdot \beta}{1+\beta}} \cdot \sqrt{\frac{2 \cdot M_y}{f_{h,1} \cdot d}} \qquad x_{2,3} = \frac{\sqrt{2}}{\sqrt{\beta \cdot (1+\beta)}} \cdot \sqrt{\frac{2 \cdot M_y}{f_{h,1} \cdot d}} \tag{17}$$

Further on applies:

$$\beta = \frac{f_{h,2}}{f_{h,1}} \qquad \psi = \frac{R_{2,VE}}{R_{1,VE}} \tag{18}$$

By placing the screws in contact with the dowels in-between the shear plane and the plastic hinges of a non-reinforced connection ($p < x_{1,3}$ and $p < x_{2,3}$) and taking into consideration the ideal rigid-plastic load-carrying behaviour of the screw loaded perpendicular to the axis, four sub-failure modes for Johansen's failure mode 3 occur (Fig. 6).

Sub-failure mode "rigid" appears for $F_{1,VE,3} < R_{1,VE}$ and $F_{2,VE,3} < R_{2,VE}$. $R_{i,VE}$ are the load-carrying capacities of the screws in both timber members. $F_{1,VE,3}$ and $F_{2,VE,3}$ are derived from the force and moment equilibrium in the shear plane for the sub-failure mode "rigid" as:

$$F_{1,VE,3} = \frac{M_y}{p} - \frac{f_{h,1} \cdot d \cdot p}{4} \cdot (3 - p) \qquad F_{2,VE,3} = \frac{M_y}{p} - \frac{f_{h,1} \cdot d \cdot p}{4} \cdot (3 \cdot \beta - 1) \tag{19}$$

In this "rigid" case, the load-carrying capacity R_3 is derived as:

$$R_3 = \frac{M_y}{p} + \frac{f_{h,1} \cdot d \cdot p}{4} \cdot (1+\beta) \tag{20}$$

The load-carrying capacity for the sub-failure mode "soft" is derived from the force and moment equilibrium in the shear plane as:

$$R_3 = R_{1,VE} \cdot \frac{(\beta+\psi)}{(1+\beta)} + \sqrt{\frac{2 \cdot \beta}{1+\beta}} \cdot \sqrt{f_{h,1} \cdot d \cdot \left(2 \cdot M_y - R_{1,VE} \cdot p \cdot (1+\psi)\right) - \frac{{R_{1,VE}}^2 \cdot (\psi - 1)^2}{2 \cdot (1+\beta)}} \tag{21}$$

This sub-failure mode appears for $p < x_{1,s,3}$ and $p < x_{2,s,3}$ (Fig. 6). The distances $x_{1,s,3}$ and $x_{2,s,3}$ can be derived from the force and moment equilibrium in the shear plane for the sub-failure mode "soft". Taking into account the assumption $p < x_{1,s,3}$ and $p < x_{2,s,3}$, following precondition for sub-failure mode "soft" is derived:

$$R_{1,VE} \le Z_3 = \min \left\{ \begin{array}{l} \frac{M_y}{p} - \frac{f_{h,1} \cdot d \cdot p}{4 \cdot \beta} \cdot (1+\beta) \\ \frac{M_y}{p} - \frac{f_{h,1} \cdot d \cdot p \cdot \beta}{4} \cdot (1+\beta) \end{array} \right\} \qquad \text{for } \psi = 1 \tag{22}$$

$$R_{1,VE} \le Z_3 = \min \left\{ \begin{array}{l} \dfrac{f_{h,1} \cdot d \cdot p}{(\psi - 1)^2} \cdot \left[\sqrt{(1+\psi)^2 \cdot (\beta^2 + \beta) - 4 \cdot \beta \cdot \psi^2 + \dfrac{4 \cdot \beta \cdot (\psi - 1)^2 \cdot M_y}{p^2 \cdot d \cdot f_{h,1}}} \right] \\ \quad -(\beta - 1) \cdot \psi - \beta - 1 \\ \dfrac{f_{h,1} \cdot d \cdot p}{(\psi - 1)^2} \cdot \left[\sqrt{(2+\psi) \cdot (\beta + 1) \cdot \psi + 1 - 3 \cdot \beta + \dfrac{4 \cdot (\psi - 1)^2 \cdot M_y}{p^2 \cdot d \cdot f_{h,1}}} \right] \\ \quad -(\beta + 1) \cdot \psi + \beta - 1 \end{array} \right\} \tag{23}$$

for $\psi \neq 1$

The load-carrying capacity for the sub-failure mode "soft-rigid" is derived from the force and moment equilibrium in the shear plane as:

$$R_3 = R_{1,VE} + f_{h,1} \cdot d \cdot \left[\sqrt{(1+\beta) \cdot p^2 - \frac{4 \cdot R_{1,VE} \cdot p - 4 \cdot M_y}{f_{h,1} \cdot d}} - p \right] \tag{24}$$

This sub-failure mode appears for $F_{1,VE,3} \cdot \psi > F_{2,VE,3}$ and for $Z < R_{1,VE} \le F_{1,VE,3}$. Those ancillary conditions can be derived in the same way from the force and moment equilibrium in the respective shear plane.

For $F_{1,VE,3} \cdot \psi \le F_{2,VE,3}$ and for $Z < R_{1,VE} \le F_{2,VE,3}/\psi$ sub-failure mode "rigid-soft" appears. The load-carrying capacity for this sub-failure mode is derived from the force and moment equilibrium in the respective shear plane as:

$$R_3 = R_{1,VE} \cdot \psi + f_{h,1} \cdot d \cdot \left[\sqrt{(1+\beta) \cdot \beta \cdot p^2 - \frac{4 \cdot \beta \cdot (R_{1,VE} \cdot \psi \cdot p - M_y)}{f_{h,1} \cdot d}} - p \cdot \beta \right] \tag{25}$$

Similarly, the other five Johansen's failure modes for reinforced timber-to-timber connections are derived.

Therewith, the load-carrying capacity for a reinforced timber-to-timber connection can be calculated as follows.

$$R = \min \{ R_{1a}, R_{1b}, R_{1c}, R_{2a}, R_{2b}, R_3 \} \tag{26}$$

with

$$R_{1a} = f_{h,1} \cdot d \cdot t_1 + R_{1,VE} \tag{27}$$

$$R_{1b} = \beta \cdot f_{h,1} \cdot d \cdot t_2 + \psi \cdot R_{1,VE} \tag{28}$$

$$R_{1c} = \frac{f_{h,1} \cdot d \cdot t_1}{(1+\beta)} \cdot \left[\sqrt{\beta + 2 \cdot \beta^2 \cdot \left(1 + \frac{t_2}{t_1} + \frac{{t_2}^2}{{t_1}^2} \right) + \beta^3 \cdot \frac{{t_2}^2}{{t_1}^2}} - \beta \cdot \left(1 + \frac{t_2}{t_1} \right) \right] \quad \begin{array}{l} \text{for } p \ge x_{1,1c} \\ \text{and } p \ge x_{2,1c} \end{array} \tag{29}$$

$$R_{1c} = \frac{f_{h,1} \cdot d \cdot t_1}{2} \cdot \left[(\beta + 1) \cdot \frac{p}{t_1} - 1 - \beta \cdot \frac{t_2}{t_1} + \left(1 + \beta \cdot \frac{{t_2}^2}{{t_1}^2} \right) \cdot \frac{t_1}{2 \cdot p} \right] \tag{30}$$

for $p < x_{1,1c}$ and $p < x_{2,1c}$ and for $R_{1,VE} > F_{1,VE,1c}$ and $R_{1,VE} > \dfrac{F_{2,VE,1c}}{\psi}$

$$R_{1c} = R_{1,VE} \cdot \frac{(\psi+\beta)}{(1+\beta)} + \frac{f_{h,1} \cdot d \cdot t_1}{(1+\beta)}$$

$$\cdot \left[\sqrt{\beta + 2 \cdot \beta^2 \cdot \left(1 + \frac{t_2}{t_1} + \frac{{t_2}^2}{{t_1}^2}\right) + \beta^3 \cdot \frac{{t_2}^2}{{t_1}^2} - \frac{{R_{1,VE}}^2 \cdot \beta \cdot (\psi-1)^2}{{t_1}^2 \cdot d^2 \cdot {f_{h,1}}^2} - \frac{2 \cdot R_{1,VE} \cdot \beta \cdot p \cdot \left(2 \cdot (1+\beta) \cdot (1+\psi) + \frac{t_1}{p} \cdot (1-\psi) \cdot \left(\beta \cdot \frac{t_2}{t_1} - 1\right)\right)}{f_{h,1} \cdot d \cdot {t_1}^2}} - \beta \cdot \left(1 + \frac{t_2}{t_1}\right) \right] \tag{31}$$

for $p < x_{1,1c}$ and $p < x_{2,1c}$ and for $R_{1,VE} \le Z_{1c}$

$$R_{1c} = R_{1,VE} + f_{h,1} \cdot d \cdot t_1$$

$$\cdot \left[\sqrt{2} \cdot \sqrt{2 \cdot \frac{p^2}{{t_1}^2} \cdot (1+\beta) + 2 \cdot \frac{p}{t_1} \cdot \left(1 - \beta \cdot \frac{t_2}{t_1}\right) + \left(1 + \beta \cdot \frac{{t_2}^2}{{t_1}^2}\right) - \frac{4 \cdot R_{1,VE} \cdot p}{{t_1}^2 \cdot d \cdot f_{h,1}}} - 2 \cdot \frac{p}{t_1} - 1 \right] \tag{32}$$

for $p < x_{1,1c}$ and $p < x_{2,1c}$ and for $F_{1,VE,1c} > \frac{F_{2,VE,1c}}{\psi}$ and $Z_{1c} < R_{1,VE} \le F_{1,VE,1c}$

$$R_{1c} = R_{1,VE} \cdot \psi + f_{h,1} \cdot d \cdot t_1 \cdot \left[\sqrt{2 \cdot \beta} \cdot \sqrt{2 \cdot \frac{p^2}{{t_1}^2} \cdot (1+\beta) - 2 \cdot \frac{p}{t_1} \cdot \left(1 - \beta \cdot \frac{t_2}{t_1}\right) + 1 + \beta \cdot \frac{{t_2}^2}{{t_1}^2} - \frac{4 \cdot R_{1,VE} \cdot \psi \cdot p}{{t_1}^2 \cdot d \cdot f_{h,1}}} - \beta \cdot \left(\frac{t_2}{t_1} + 2 \cdot \frac{p}{t_1}\right) \right] \tag{33}$$

for $p < x_{1,1c}$ and $p < x_{2,1c}$ and for $F_{1,VE,1c} \le \frac{F_{2,VE,1c}}{\psi}$ and $Z_{1c} < R_{1,VE} \le \frac{F_{2,VE,1c}}{\psi}$

With

$$x_{1,1c} = \frac{t_1}{2 \cdot (1+\beta)} \cdot \left[\sqrt{\beta + 2 \cdot \beta^2 \cdot \left[1 + \frac{t_2}{t_1} + \left(\frac{t_2}{t_1}\right)^2\right] + \beta^3 \cdot \left(\frac{t_2}{t_1}\right)^2} + 1 - \beta \cdot \frac{t_2}{t_1} \right] \tag{34}$$

$$x_{2,1c} = \frac{t_1}{2 \cdot \beta \cdot (1+\beta)} \cdot \left[\sqrt{\beta + 2 \cdot \beta^2 \cdot \left[1 + \frac{t_2}{t_1} + \left(\frac{t_2}{t_1}\right)^2\right] + \beta^3 \cdot \left(\frac{t_2}{t_1}\right)^2} - \beta \cdot \left(1 - \beta \cdot \frac{t_2}{t_1}\right) \right] \tag{35}$$

$$F_{1,VE,1c} = \frac{f_{h,1} \cdot d \cdot t_1}{2} \cdot \left[(\beta - 3) \cdot \frac{p}{t_1} + 1 - \beta \cdot \frac{t_2}{t_1} + \left(1 + \beta \cdot \frac{{t_2}^2}{{t_1}^2}\right) \cdot \frac{t_1}{2 \cdot p} \right] \tag{36}$$

$$F_{2,VE,1c} = \frac{f_{h,1} \cdot d \cdot t_1}{2} \cdot \left[(1 - 3 \cdot \beta) \cdot \frac{p}{t_1} - 1 + \beta \cdot \frac{t_2}{t_1} + \left(1 + \beta \cdot \frac{{t_2}^2}{{t_1}^2}\right) \cdot \frac{t_1}{2 \cdot p} \right] \tag{37}$$

$$Z_{1c} = \min\left\{ \begin{array}{l} \dfrac{\mathrm{f_{h,1}}\cdot d}{(\psi-1)^2}\cdot\left[\begin{array}{l}(t_1 - t_2\cdot\beta - 2\cdot p)\cdot(1-\psi) - 2\cdot p\cdot\beta\cdot(1+\psi) + \sqrt{2\cdot\beta} \\ \cdot\sqrt{\begin{array}{l}2\cdot p^2\cdot(\psi+1)^2\cdot(1+\beta) + {t_1}^2\cdot(\psi-1)^2\cdot\left(1+\beta\cdot\dfrac{{t_2}^2}{{t_1}^2}\right) \\ +2\cdot p\cdot t_1\cdot(1-\psi^2)\cdot\left(\beta\cdot\dfrac{t_2}{t_1}-1\right) - 8\cdot\psi^2\cdot p^2\end{array}}\end{array}\right] \\ \dfrac{\mathrm{f_{h,1}}\cdot d}{(\psi-1)^2}\cdot\left[\begin{array}{l}(t_1 - t_2\cdot\beta - 2\cdot p)\cdot(1-\psi) + 2\cdot p\cdot\beta\cdot(1-\psi) - 4\cdot\psi\cdot p \\ +\sqrt{2}\cdot\sqrt{\begin{array}{l}2\cdot p^2\cdot\psi\cdot(\psi+2)\cdot(1+\beta) + 2\cdot p^2\cdot(1-3\cdot\beta) \\ +2\cdot p\cdot(1-\psi^2)\cdot(\beta\cdot t_2 - t_1) + (\psi-1)^2\cdot({t_1}^2 + \beta\cdot{t_2}^2)\end{array}}\end{array}\right] \end{array}\right\} \tag{38}$$

for $\psi \neq 1$

$$Z_{1c} = \min\left\{ \begin{array}{l} \dfrac{f_{h,1}\cdot d}{2\cdot\beta}\cdot\left[(t_1 - t_2\cdot\beta) - p\cdot(\beta+1) + \dfrac{{t_1}^2}{2\cdot p}\cdot(\beta-1) + \dfrac{(\beta\cdot t_2 + t_1)^2}{4\cdot p}\right] \\ \dfrac{f_{h,1}\cdot d\cdot\beta}{2}\cdot\left[(t_2\cdot\beta - t_1) - p\cdot(\beta+1) + \dfrac{{t_2}^2}{2\cdot p}\cdot(1-\beta) + \dfrac{(\beta\cdot t_2 + t_1)^2}{4\cdot p\cdot\beta}\right] \end{array}\right\} \tag{39}$$

for $\psi = 1$

$$R_{2a} = \frac{f_{h,1}\cdot d\cdot t_1}{(2+\beta)}\cdot\left[\sqrt{2\cdot\beta\cdot(1+\beta) + \frac{4\cdot\beta\cdot(2+\beta)\cdot M_y}{f_{h,1}\cdot d\cdot {t_1}^2}} - \beta\right] \qquad \begin{array}{l}\text{for } p \geq x_{1,2a} \\ \text{and } p \geq x_{2,2a}\end{array} \tag{40}$$

$$R_{2a} = \frac{f_{h,1}\cdot d\cdot t_1}{4}\cdot\left[(\beta+2)\cdot\frac{p}{t_1} - 2 + \frac{t_1}{p}\right] + \frac{M_y}{2\cdot p} \tag{41}$$

for $p < x_{1,2a}$ and $p < x_{2,2a}$ and for $R_{1,VE} > F_{1,VE,2a}$ and $R_{1,VE} > \dfrac{F_{2,VE,2a}}{\psi}$

$$R_{2a} = R_{1,VE}\cdot\frac{(2\cdot\psi+\beta)}{(2+\beta)} + \frac{f_{h,1}\cdot d\cdot t_1}{(2+\beta)}\cdot\left[\sqrt{\begin{array}{l}2\cdot\beta\cdot(1+\beta) - \dfrac{2\cdot {R_{1,VE}}^2\cdot\beta\cdot(\psi-1)^2}{{t_1}^2\cdot d^2\cdot {f_{h,1}}^2} \\ -\dfrac{4\cdot R_{1,VE}\cdot\beta\cdot\left(\dfrac{p}{t_1}\cdot(1+\psi)\cdot(2+\beta) + \psi - 1\right)}{f_{h,1}\cdot d\cdot t_1} + \dfrac{4\cdot\beta\cdot(2+\beta)\cdot M_y}{f_{h,1}\cdot d\cdot {t_1}^2}\end{array}} - \beta\right] \tag{42}$$

for $p < x_{1,2a}$ and $p < x_{2,2a}$ and for $R_{1,VE} \leq Z_{2a}$

$$R_{2a} = R_{1,VE} + f_{h,1} \cdot d \cdot t_1 \cdot \left[\sqrt{(2+\beta) \cdot 2 \cdot \frac{p^2}{t_1^2} + 2 + 4 \cdot \frac{p}{t_1} - \frac{\left(8 \cdot R_{1,VE} \cdot p - 4 \cdot M_y\right)}{t_1^2 \cdot f_{h,1} \cdot d}} - 2 \cdot \frac{p}{t_1} - 1 \right] \tag{43}$$

for $p < x_{1,2a}$ and $p < x_{2,2a}$ and for $F_{1,VE,2a} > \frac{F_{2,VE,2a}}{\psi}$ and $Z_{2a} < R_{1,VE} \le F_{1,VE,2a}$

$$R_{2a} = R_{1,VE} \cdot \psi + f_{h,1} \cdot d \cdot t_1 \cdot \left[\sqrt{(2+\beta) \cdot \beta \cdot \frac{p^2}{t_1^2} + \beta - 2 \cdot \beta \cdot \frac{p}{t_1} - \frac{\beta \cdot \left(4 \cdot R_{1,VE} \cdot \psi \cdot p - 2 \cdot M_y\right)}{t_1^2 \cdot f_{h,1} \cdot d}} - \beta \cdot \frac{p}{t_1} \right] \tag{44}$$

for $p < x_{1,2a}$ and $p < x_{2,2a}$ and for $F_{1,VE,2a} \le \frac{F_{2,VE,2a}}{\psi}$ and $Z_{2a} < R_{1,VE} \le \frac{F_{2,VE,2a}}{\psi}$

$$x_{1,2a} = \frac{t_1}{2 \cdot (2+\beta)} \cdot \left[\sqrt{2 \cdot \beta \cdot (1+\beta) + \frac{(2+\beta) \cdot \beta \cdot 4 \cdot M_y}{t_1^2 \cdot f_{h,1} \cdot d}} + 2 \right] \tag{45}$$

$$x_{2,2a} = \frac{t_1}{\beta \cdot (2+\beta)} \cdot \left[\sqrt{2 \cdot \beta \cdot (1+\beta) + \frac{(2+\beta) \cdot \beta \cdot 4 \cdot M_y}{t_1^2 \cdot f_{h,1} \cdot d}} - \beta \right] \tag{46}$$

$$F_{1,VE,2a} = \frac{f_{h,1} \cdot d \cdot t_1}{4} \cdot \left[(\beta - 6) \cdot \frac{p}{t_1} + 2 + \frac{t_1}{p} \right] + \frac{M_y}{2 \cdot p} \tag{47}$$

$$F_{2,VE,2a} = \frac{f_{h,1} \cdot d \cdot t_1}{4} \cdot \left[(2 - 3 \cdot \beta) \cdot \frac{p}{t_1} - 2 + \frac{t_1}{p} \right] + \frac{M_y}{2 \cdot p} \tag{48}$$

$$Z_{2a} = \min \left\{ \begin{array}{l} \frac{f_{h,1} \cdot d}{(\psi - 1)^2} \cdot \left[\begin{array}{l} (2 \cdot p - t_1 - \beta \cdot p) \cdot (\psi - 1) - 2 \cdot p \cdot \beta \\ + \sqrt{\begin{array}{l} \beta \cdot p^2 \cdot (\psi + 1)^2 \cdot (2+\beta) + 2 \cdot p \cdot t_1 \cdot \beta \cdot (\psi^2 - 1) \\ + \beta \cdot t_1^2 \cdot (\psi - 1)^2 - 8 \cdot \beta \cdot \psi^2 \cdot p^2 + \frac{2 \cdot \beta \cdot (\psi - 1)^2 \cdot M_y}{f_{h,1} \cdot d} \end{array}} \end{array} \right] \\ \frac{f_{h,1} \cdot d}{(\psi - 1)^2} \cdot \left[\begin{array}{l} (2 \cdot p + t_1 + \beta \cdot p) \cdot (1 - \psi) - 4 \cdot p \\ + \sqrt{2} \cdot \sqrt{\begin{array}{l} p^2 \cdot (\psi + 1)^2 \cdot (2+\beta) + 2 \cdot p \cdot t_1 \cdot (\psi^2 - 1) \\ + t_1^2 \cdot (\psi - 1)^2 - 4 \cdot \beta \cdot p^2 + \frac{2 \cdot (\psi - 1)^2 \cdot M_y}{f_{h,1} \cdot d} \end{array}} \end{array} \right] \end{array} \right\} \tag{49}$$

for $\psi \neq 1$

$$Z_{2a} = \min \left\{ \begin{array}{l} \frac{f_{h,1} \cdot d}{4 \cdot p \cdot \beta} \cdot \left[(\beta - 1) \cdot t_1^2 + 4 \cdot p \cdot t_1 - 2 \cdot p^2 \cdot (2+\beta) \right] + \frac{M_y}{2 \cdot p} \\ \frac{f_{h,1} \cdot d}{8 \cdot p} \cdot \left[t_1^2 - 2 \cdot p \cdot \beta \cdot t_1 - p^2 \cdot \beta \cdot (2+\beta) \right] + \frac{M_y}{2 \cdot p} \end{array} \right\} \text{ for } \psi = 1 \tag{50}$$

$$R_{2b} = \frac{f_{h,1} \cdot d \cdot t_2}{(2 \cdot \beta + 1)} \cdot \left[\sqrt{2 \cdot \beta^2 \cdot (1 + \beta) + \frac{4 \cdot \beta \cdot (2 \cdot \beta + 1) \cdot M_y}{f_{h,1} \cdot d \cdot {t_2}^2}} - \beta \right] \qquad \begin{matrix} \text{for } p \geq x_{1,2b} \\ \text{and } p \geq x_{2,2b} \end{matrix} \tag{51}$$

$$R_{2b} = \frac{f_{h,1} \cdot d \cdot t_2}{4} \cdot \left[(2 \cdot \beta + 1) \cdot \frac{p}{t_2} + 2 \cdot \beta \cdot \left(\frac{t_2}{2 \cdot p} - 1 \right) \right] + \frac{M_y}{2 \cdot p} \tag{52}$$

for $p < x_{1,2b}$ and $p < x_{2,2b}$ and for $R_{1,VE} > F_{1,VE,2b}$ and $R_{1,VE} > \frac{F_{2,VE,2b}}{\psi}$

$$R_{2b} = R_{1,VE} \cdot \frac{(2 \cdot \beta + \psi)}{(2 \cdot \beta + 1)} + \frac{f_{h,1} \cdot d \cdot t_2}{(2 \cdot \beta + 1)} \cdot \left[\sqrt{2 \cdot \beta^2 \cdot (1 + \beta) - \frac{2 \cdot {R_{1,VE}}^2 \cdot \beta \cdot (\psi - 1)^2}{{t_2}^2 \cdot d^2 \cdot {f_{h,1}}^2} + \frac{4 \cdot \beta \cdot (2 \cdot \beta + 1) \cdot M_y}{f_{h,1} \cdot d \cdot {t_2}^2}} - \frac{4 \cdot R_{1,VE} \cdot \beta \cdot \left(\frac{p}{t_2} \cdot (1 + \psi) \cdot (2 \cdot \beta + 1) + \beta - \psi \cdot \beta \right)}{f_{h,1} \cdot d \cdot t_2} - \beta \right] \tag{53}$$

for $p < x_{1,2b}$ and $p < x_{2,2b}$ and for $R_{1,VE} \leq Z_{2b}$

$$R_{2b} = R_{1,VE} + f_{h,1} \cdot d \cdot t_2 \cdot \left[\sqrt{(1 + 2 \cdot \beta) \cdot \frac{p^2}{{t_2}^2} + \left(1 - 2 \cdot \frac{p}{t_2} \right) \cdot \beta - \frac{\left(4 \cdot R_{1,VE} \cdot p - 2 \cdot M_y \right)}{{t_2}^2 \cdot f_{h,1} \cdot d}} - \frac{p}{t_2} \right] \tag{54}$$

for $p < x_{1,2b}$ and $p < x_{2,2b}$ and for $F_{1,VE,2b} > \frac{F_{2,VE,2b}}{\psi}$ and $Z_{2b} < R_{1,VE} \leq F_{1,VE,2b}$

$$R_{2b} = R_{1,VE} \cdot \psi + f_{h,1} \cdot d \cdot t_2 \cdot \left[\sqrt{\beta} \cdot \sqrt{(1 + 2 \cdot \beta) \cdot 2 \cdot \frac{p^2}{{t_2}^2} + \left(1 + 2 \cdot \frac{p}{t_2} \right) \cdot 2 \cdot \beta - \frac{4 \cdot \left(2 \cdot R_{1,VE} \cdot \psi \cdot p - M_y \right)}{{t_2}^2 \cdot f_{h,1} \cdot d}} - \beta \cdot \left(1 + 2 \cdot \frac{p}{t_2} \right) \right] \tag{55}$$

for $p < x_{1,2b}$ and $p < x_{2,2b}$ and for $F_{1,VE,2b} \leq \frac{F_{2,VE,2b}}{\psi}$ and $Z_{2b} < R_{1,VE} \leq \frac{F_{2,VE,2b}}{\psi}$

With

$$x_{1,2b} = \frac{t_2}{1 + 2 \cdot \beta} \cdot \left[\sqrt{2 \cdot \beta^2 \cdot (1 + \beta) + \frac{(1 + 2 \cdot \beta) \cdot \beta \cdot 4 \cdot M_y}{{t_2}^2 \cdot f_{h,1} \cdot d}} - \beta \right] \tag{56}$$

$$x_{2,2b} = \frac{t_2}{2 \cdot \beta \cdot (1 + 2 \cdot \beta)} \cdot \left[\sqrt{2 \cdot \beta^2 \cdot (1 + \beta) + \frac{(1 + 2 \cdot \beta) \cdot \beta \cdot 4 \cdot M_y}{{t_2}^2 \cdot f_{h,1} \cdot d}} + 2 \cdot \beta^2 \right] \tag{57}$$

$$F_{1,VE,2b} = \frac{f_{h,1} \cdot d \cdot t_2}{4} \cdot \left[(2 \cdot \beta - 3) \cdot \frac{p}{t_2} + 2 \cdot \beta \cdot \left(\frac{t_2}{2 \cdot p} - 1 \right) \right] + \frac{M_y}{2 \cdot p} \tag{58}$$

$$F_{2,VE,2b} = \frac{f_{h,1} \cdot d \cdot t_2}{4} \cdot \left[(1 - 6 \cdot \beta) \cdot \frac{p}{t_2} + 2 \cdot \beta \cdot \left(\frac{t_2}{2 \cdot p} + 1 \right) \right] + \frac{M_y}{2 \cdot p} \tag{59}$$

$$Z_{2b} = \min \left\{ \begin{array}{l} \dfrac{\mathrm{f}_{\mathrm{h},1} \cdot d}{(\psi - 1)^2} \cdot \left[\begin{array}{l} (p + \beta \cdot t_2 - 2 \cdot \beta \cdot p) \cdot (\psi - 1) - 4 \cdot p \cdot \beta + \sqrt{2} \\ \cdot \sqrt{\begin{array}{l} \beta \cdot p^2 \cdot (\psi + 1)^2 \cdot (2 \cdot \beta + 1) + 2 \cdot p \cdot t_2 \cdot \beta^2 \cdot (1 - \psi^2) \\ + \beta^2 \cdot {t_2}^2 \cdot (\psi - 1)^2 - 4 \cdot \beta \cdot \psi^2 \cdot p^2 + \dfrac{2 \cdot \beta \cdot (\psi - 1)^2 \cdot M_y}{\mathrm{f}_{\mathrm{h},1} \cdot d} \end{array}} \end{array} \right] \\ \dfrac{\mathrm{f}_{\mathrm{h},1} \cdot d}{(\psi - 1)^2} \cdot \left[\begin{array}{l} (2 \cdot p \cdot \beta - \beta \cdot t_2 + p) \cdot (1 - \psi) - 2 \cdot p \\ + \sqrt{\begin{array}{l} p^2 \cdot (\psi + 1)^2 \cdot (2 \cdot \beta + 1) + 2 \cdot \beta \cdot p \cdot t_2 \cdot (1 - \psi^2) \\ + \beta \cdot {t_2}^2 \cdot (\psi - 1)^2 - 8 \cdot \beta \cdot p^2 + \dfrac{2 \cdot (\psi - 1)^2 \cdot M_y}{\mathrm{f}_{\mathrm{h},1} \cdot d} \end{array}} \end{array} \right] \end{array} \right\} \tag{60}$$

for $\psi \neq 1$

$$Z_{2b} = \min \left\{ \begin{array}{l} \dfrac{f_{h,1} \cdot d}{8 \cdot p \cdot \beta} \cdot \left[\beta^2 \cdot {t_2}^2 - 2 \cdot p \cdot \beta \cdot t_2 - p^2 \cdot (2 \cdot \beta + 1) \right] + \dfrac{M_y}{2 \cdot p} \\ \dfrac{f_{h,1} \cdot d}{4 \cdot p} \cdot \left[4 \cdot p \cdot \beta^2 \cdot t_2 - 2 \cdot p^2 \cdot \beta \cdot (2 \cdot \beta + 1) + {t_2}^2 \cdot \beta \cdot (1 - \beta) \right] + \dfrac{M_y}{2 \cdot p} \end{array} \right\} \tag{61}$$

for $\psi = 1$

The load-carrying capacity R_3 for failure mode 3 is calculated according to the equations (16) to (25).

Fig. 7 shows the reinforcing effect as a R over $R_{1,VE}$ diagram for a timber-to-timber connection with a 16 mm dowel, for an embedding strength $f_{h,1}$ = 26 N/mm^2, a yield moment M_y = 246 Nm, timber member thicknesses t_1 = 60 mm and t_2 = 80 mm and for a distance p = 15 mm (β = 1,2; ψ = 1,1).

For $R_{1,VE}$ = 0 the load carrying capacity R is equal to the load-carrying capacity for a non-reinforced connection (R = 12,4 kN). Here, failure mode 2a with one plastic hinge in the right timber member occurs. With increasing load-carrying capacity $R_{1,VE}$ (and $R_{2,VE}$) of the screws, the load-carrying capacity R of the timber-to-timber connection increases. For $R_{1,VE}$ = 15,3 kN and $R_{2,VE} = \psi \cdot R_{1,VE}$ = 16,8 kN the load-carrying capacity R reaches the maximum value of R = 19,8 kN which corresponds to an increase of about 60%. Due to the fact that for higher values of R_{VE} sub-failure mode “rigid” occurs, a further increase is not possible for this configuration.

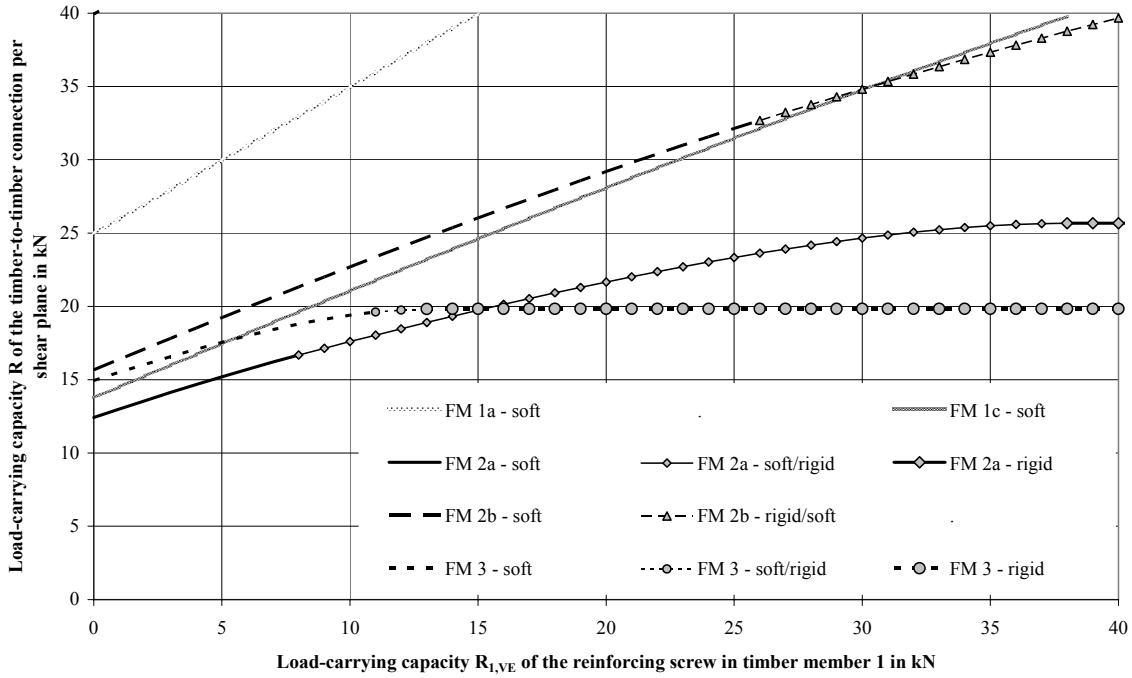

Fig. 7: Load-carrying capacity R of a timber-to-timber connection depending on $R_{1,VE}$

2.4 Load-carrying capacity of the reinforcements

The load-carrying capacity R of reinforced connections is calculated depending on the load-carrying capacity $R_{i,VE}$ of the reinforcing screws. $R_{i,VE}$ is derived and calculated according to Johansen´s yield theory as for steel-to-timber connections with inner steel plates. For the case of one dowel-type fastener being reinforced by one screw (Fig. 8), the load-carrying capacity R_{VE} follows as:

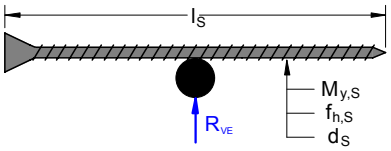

$$R_{VE} = \min\left\{R_{A1}, R_{A2}, R_{A3}\right\} \tag{62}$$

Fig. 8: One dowel-type fastener reinforced by one screw

$$R_{A1} = f_{h,S} \cdot d_S \cdot l_S \tag{63}$$

$$R_{A2} = f_{h,S} \cdot d_S \cdot l_S \cdot \left[\sqrt{\frac{16 \cdot M_{y,S}}{f_{h,S} \cdot d_S \cdot {l_S}^2} + 2} - 1\right] \tag{64}$$

$$R_{A3} = 4 \cdot \sqrt{M_{y,S} \cdot f_{h,S} \cdot d_S} \tag{65}$$

Six possible failure modes must be taken into consideration when two adjacent dowel-type fasteners are reinforced by one screw (Fig. 9).

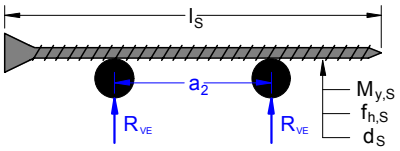

$$R_{VE} = \min\left\{R_{B1}, R_{B2}, R_{B3}, R_{B4}, R_{B5}, R_{B6}\right\} \tag{66}$$

Fig. 9: Two dowel-type fasteners reinforced by one screw

$$R_{B1} = 0{,}5 \cdot f_{h,S} \cdot d_S \cdot l_S \tag{67}$$

$$R_{B2} = \frac{f_{h,S} \cdot d_S \cdot l_S}{2} \cdot \left[\sqrt{\frac{16 \cdot M_{y,S}}{f_{h,S} \cdot d_S \cdot l_S^{\,2}} + 2 \cdot \left(\frac{a_2}{l_S} - 1\right)^2} + 2 \cdot \frac{a_2}{l_S} - 1\right] \tag{68}$$

$$R_{B3} = \frac{f_{h,S} \cdot d_S \cdot a_2}{2} + \sqrt{2} \cdot \sqrt{2 \cdot M_{y,S} \cdot f_{h,S} \cdot d_S} \tag{69}$$

$$R_{B4} = 4 \cdot \sqrt{M_{y,S} \cdot f_{h,S} \cdot d_S} \tag{70}$$

$$R_{B5} = \frac{f_{h,S} \cdot d_S \cdot l_S}{2} \cdot \left[\sqrt{\frac{16 \cdot M_{y,S}}{f_{h,S} \cdot d_S \cdot l_S^{\,2}} + 2 \cdot \left(\frac{a_2}{l_S} - 1\right)^2} + 4 \cdot \sqrt{\frac{M_{y,S}}{f_{h,S} \cdot d_S \cdot l_S^{\,2}}} + \frac{a_2}{l_S} - 1\right] \tag{71}$$

$$R_{B6} = \frac{f_{h,S} \cdot d_S \cdot l_S}{2} \cdot \left[\sqrt{\frac{8 \cdot M_{y,S}}{f_{h,S} \cdot d_S \cdot l_S^{\,2}} + \left(\frac{a_2}{l_S} - 1\right)^2} - \frac{a_2}{l_S} + 1\right] \tag{72}$$

If more than two dowel-type fasteners are reinforced by one screw, the load-carrying capacity R_{VE} can be derived by combining eq. (62) with eq. (66).

2.5 Tests

In order to confirm the extended Johansen´s yield theory for reinforced connections, tests with reinforced and non-reinforced steel-to-timber and timber-to-timber connections were performed. For each test series five reinforced and five non-reinforced specimens were tested. All parameters and test results are summarised in Table 1. The specimen notation is displayed in column one. Reinforced and non-reinforced steel-to-timber connections with inner steel plates, two shear planes and dowels as fasteners are listed in lines one to six. In the following four lines reinforced and non-reinforced steel-to-timber connections with outer steel plates, two shear planes and bolts as fasteners are shown. The following lines contain the main parameters for further timber-to-timber connections. Columns five to nine contain the connection geometry and the parameters of the dowel-type fasteners. The properties of the reinforcements are described in column ten to fifteen. In column sixteen the average load-carrying capacity per shear plane and dowel-type fastener for each test series is shown.

Table 1: Specimens parameters and test results

Specimen	Number of specimens n [-]	Type [-]	mean density ρ [kg/m³]	Dowel-type fasteners					Reinforcements						load-carrying capacity R_{VM} [kN]
				t_1 [mm]	t_2 [mm]	d [mm]	M_y [Nm]	number of dowels perpendic./ parallel to grain	d_S [mm]	l_S [mm]	distance p [mm]	a_2 [mm]	R_{VE} [kN]	number of screws [-]	
S-2-8-0	5	T-S-T	412	60		8	51,2	2 / 1	-	-	-	40		-	**7,65**
S-2-8-1	5	T-S-T	425	60		8	51,2	2 / 1	7,5	130	15	40	7,21	1	**9,33**
S-1-16-0	5	T-S-T	406	60		16	164	1 / 1	-	-	-	-		-	**16,1**
S-1-16-1	5	T-S-T	416	60		16	164	1 / 1	7,5	130	15	-	9,26	1	**22,6**
S-1-24-0	5	T-S-T	396	60		24	553	1 / 1	-	-	-	-		-	**32,0**
S-1-24-2	5	T-S-T	407	60		24	553	1 / 1	7,5	130	15	-	9,13	2	**53,5**
B-2-8-0	5	S-T-S	397	60		8	36,7	2 / 1	-	-	-	40		-	**6,38**
B-2-8-2	5	S-T-S	401	60		8	36,7	2 / 1	7,5	130	15	40	6,77	2	**12,6**
B-1-20-0	5	S-T-S	411	60		20	573	1 / 1	-	-	-	-		-	**16,9**
B-1-20-2	5	S-T-S	414	60		20	573	1 / 1	7,5	130	15	-	9,22	2	**31,2**
H-24-0	5	T-T	412	50	50	24	553	1 / 2	-	-	-	-		-	**13,1**
H-24-1	5	T-T	409	50	50	24	553	1 / 2	7,5	180	15	-	9,15	1	**19,1**
H-16-0	5	T-T	415	40	40	16	164	2 / 2	-	-	-	60		-	**7,6**
H-16-1	5	T-T	399	40	40	16	164	2 / 2	7,5	180	15	60	9,01	1	**11,5**
H-20-0	5	T-T-T	392	100	60	20	320	2 / 2	-	-	-	60		-	**19,6**
H-20-1	5	T-T-T	403	100	60	20	320	2 / 2	7,5	180	15	60	9,07	1	**24,5**
H-30-0	5	T-T-T	415	100	100	30	1080	1 / 2	-	-	-	-		-	**34,9**
H-30-1	5	T-T-T	408	100	100	30	1080	1 / 2	7,5	180	15	-	9,14	1	**42,3**

The expected load-carrying capacities for each test series were calculated using the average timber density, fastener yield moment and the connection geometry. The comparison between test results and calculated load-carrying capacities is shown in Fig. 10.

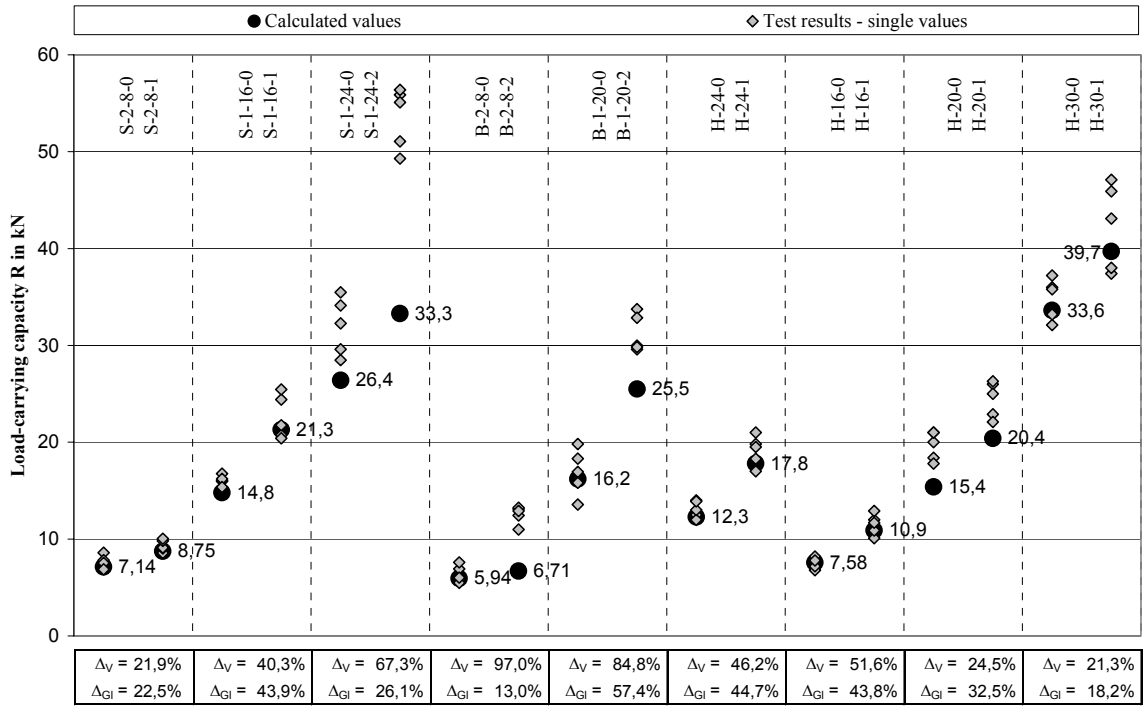

Fig. 10: Comparison between test results and calculated load-carrying capacities

On the left side in each column the load-carrying capacities of non-reinforced connections are shown. The load-carrying-capacities of geometrically identical reinforced connections are displayed on the right side. In the bottom line the calculated increases Δ_{Gl} and Δ_v reached in tests compared to non-reinforced connections are displayed. For the test series

in column 1, 2, 6 to 9, the calculated increases are similar to the increases reached in tests. For the test series in column 3 to 5, the increase reached in tests are clearly larger than the calculated increases. The reason for this discrepancy is the number of the reinforcements for each dowel-type fastener. In the latter, each dowel-type fastener was reinforced by two parallel screws. The presented calculation model is valid for connections reinforced with one screw per one or two dowels. This particular case with two screws per dowel can be derived similarly to the presented calculation model or conservatively be handled with the presented method.

An opened steel-to-timber connection is shown in Fig. 11. On the left side the non-reinforced connection S-2-8-0 and on the right side the reinforced connection S-2-8-1 is displayed. The load-carrying capacities reached in tests and even the failure modes were calculated using the extended Johansen´s yield theory.

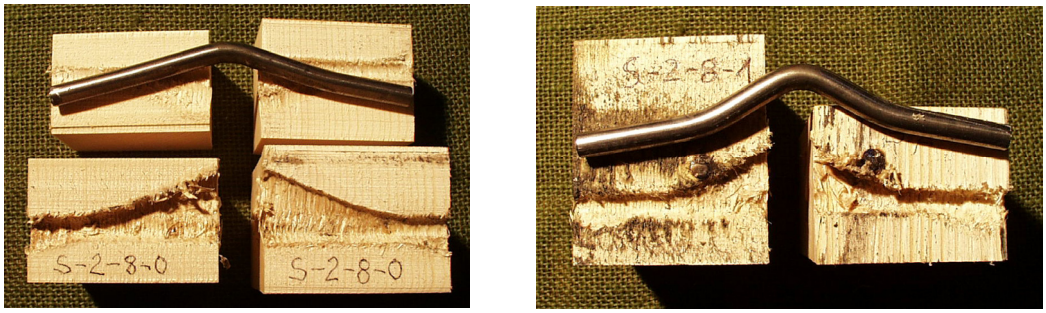

Fig. 11: Left: non-reinforced connection S-2-8-0 – Right: reinforced connection S-2-8-1

In Fig. 12 two opened reinforced steel-to-timber connections S-1-24-2 and S-1-16-1 as well as a non-reinforced connection S-1-16-0 are displayed. In both pictures the sub-failure mode “soft” dominates the failure.

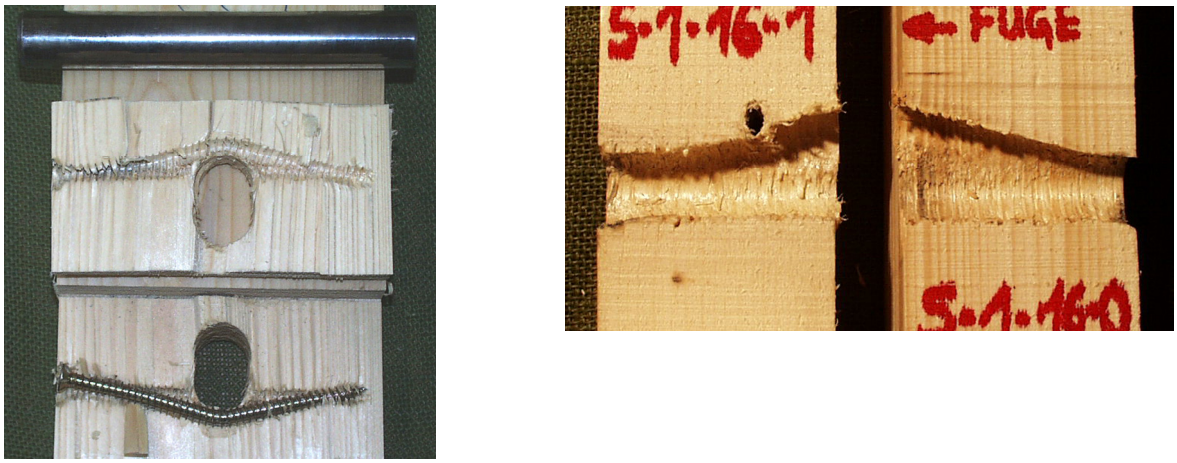

Fig. 12: Left: reinforced connection S-1-24-2 – Right: reinforced and non-reinforced connection S-1-16-1 and S-1-16-0

For numerous reinforced connections a parameter study was performed. The influence of the ratio of the reinforcement diameter d_S to the dowel diameter d on the increase of the load-carrying capacity was studied. Thereby all parameters plausible for practical application were varied. Depending on the diameter d_S of the reinforcement and on the diameter d of the dowel, the increase due to the reinforcement is shown in Fig. 13. In this comparison the influence of brittle timber splitting was not taken into account ($n = n_{ef}$).

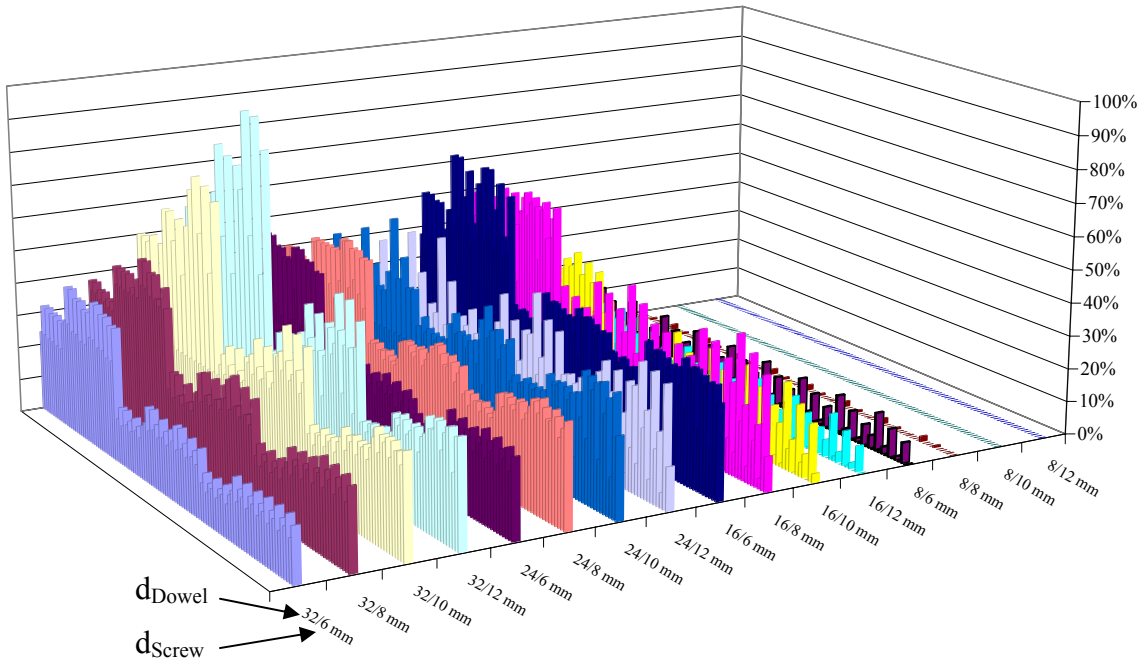

Fig.13: Increase of the load-carrying capacity for a reinforced connection compared to a non-reinforced connection without taking into account the timber splitting

Considering this parameter study, the largest increase can be reached in connections with dowel-type fasteners with a large diameter d. The largest reinforcement effect was reached in connections with dowel-fasteners with 32 mm diameter. Further on, the largest increasing effect can be reached for a ratio of the screw diameter d_S to the dowel diameter d of about d_S / d = 0,35 to 0,40. The largest increase was calculated to about 80%. Here again, the brittle splitting behaviour was not taken into account ($n = n_{ef}$).

3 Summary

Self-tapping screws with continuous thread represent a simple and economic method to reinforce connections where the timber is prone to splitting. In connections with sufficient reinforcement between the dowels, the timber does not split and the effective number n_{ef} equals the actual number n of dowels. Furthermore, by placing the screws in contact with the dowel-type fasteners, the load-carrying capacity and the stiffness of a connection increases.

A calculation model based on Johansen´s yield theory was developed. Depending on the embedding strength of the timber, the yield moment of the dowel-type fasteners, the geometry of the connection and finally on the load-carrying capacity of the reinforcements, the load-carrying capacity of reinforced connections can be calculated.

This reinforcing method causes an increase of the load-carrying capacity up to 80% compared to non-reinforced connections with a ductile load-carrying behaviour. Compared to non-reinforced connections with a brittle load-carrying behaviour ($n_{ef} < n$), the method shows an increase of the load-carrying capacity of up to 120%.

Both values were verified by tests.

4 References

[1] Schmid, M. (2002). Anwendung der Bruchmechanik auf Verbindungen mit Holz. 5. Folge – Heft 7. Berichte der Versuchsanstalt für Stahl, Holz und Steine der Universität Fridericiana in Karlsruhe (TH):

[2] Blaß, H.J.; Ehlbeck, J.; Kreuzinger, H.; Steck, G. (2002). Entwurf, Berechnung und Bemessung von Holzbauwerken, BEKS 1-16 und Anhänge (13.07.2002); In: Ingenieurholzbau – Karlsruher Tage 2002; Bruderverlag; Universität Karlsruhe (TH)

[3] Bejtka, I. (2005). Verstärkung von Bauteilen aus Holz mit Vollgewindeschrauben. Band 2 der Reihe Karlsruher Berichte zum Ingenieurholzbau. Herausgeber: Universität Karlsruhe (TH), Lehrstuhl für Ingenieurholzbau und Baukonstruktionen, Univ.-Prof. Dr.-Ing. H.J. Blaß. ISSN 1860-093X,ISBN 3-937300-54-6